Bqt2p is essential for initiating telomere clustering upon pheromone sensing in fission yeast

Xie Tang, Ye Jin, and W. Zacheus Cande

Department of Molecular and Cell Biology, University of California, Berkeley, Berkeley, CA 94720

The telomere bouquet, i.e., telomere clustering on the nuclear envelope (NE) during meiotic prophase, is thought to promote homologous chromosome pairing. Using a visual screen, we identified *bqt2/im295*, a mutant that disrupts telomere clustering in fission yeast. Bqt2p is required for linking telomeres to the meiotic spindle pole body (SPB) but not for attachment of telomeres or the SPB to the NE. Bqt2p is expressed upon pheromone sensing and colocalizes thereafter to Sad1p, an SPB protein. This localization only depends on Bqt1p, not on other identified proteins required for telomere clustering. Upon pheromone sensing, generation of Sad1p foci next to telomeres depends on Bqt2p. However, depletion of Bqt2p from the SPB is dispensable for dissolving the telomere bouquet at the end of meiotic prophase. Therefore, telomere bouquet formation requires Bqt2p as a linking component and is finely regulated during meiotic progression.

Introduction

Homologous pairing during meiotic prophase is essential for homologous recombination and for chromosome segregation during meiosis I; yet, it is largely unknown how homologues approach each other. A chromosomal rearrangement called the telomere bouquet in early meiotic prophase is thought to play a key role in homologous pairing (Scherthan, 2001; Harper et al., 2004). It forms as telomeres cluster to a small region on the nuclear envelope (NE). Though the telomere bouquet is conserved in most organisms, the mechanism of its formation is not well understood.

Fission yeast, *Schizosaccharomyces pombe*, serves as a good model organism to study telomere bouquet formation because it has a conspicuous method for clustering telomeres. Telomeres are in subclusters scattered on the inner NE in mitotic cells and reorganized upon pheromone sensing (Chikashige et al., 1997), as telomeres start to cluster on the NE adjacent to the SPB. Such reorganization persists during premeiotic S phase and meiotic prophase, as the horsetail-shaped nucleus is driven back and forth by the microtubule arrays attached to the SPB. Therefore, the telomere bouquet could help the homologues approach each other, and the horsetail movement stretches them to facilitate their alignment.

Although many proteins have been identified in the telomere complex and the SPB, the linking components between them for bouquet formation are not well understood, and the forces that cluster telomeres have not been described. Rap1p is a telomere binding protein that is essential for telomere clustering (Chikashige and Hiraoka, 2001; Kanoh and Ishikawa, 2001). Sad1p, a spindle pole body (SPB) protein (Hagan and Yanagida, 1995) could function as a transmembrane linker for the bouquet formation. It has a transmembrane domain and a Sad1/UNC-like domain, which is an essential part of the UNC-84 protein for nuclear migration in *Caenorhabditis elegans* (Lee et al., 2002). These two domains are also in the SPB half-bridge protein Mps3p/Nep98p (Nishikawa et al., 2003), the reciprocal best hit with Sad1p in budding yeast. Furthermore, Sad1p interacts with Kms1p (Miki et al., 2004), a protein that is required for telomere clustering (Shimanuki et al., 1997), and with dynein light chain Dlc1p, which is required for the horsetail movement (Miki et al., 2002). Cytoplasmic microtubules are thought to be involved in clustering telomeres in fission yeast. However, this may not be the case in other organisms.

To identify more genes for bouquet formation, we developed a visual screen by monitoring heterochromatin reorganization upon meiosis. One mutant we found, *im295*, was defective in bouquet formation and was an allele to *bqt2* that was identified in genome-wide screens by systematically deleting upregulated genes during meiotic prophase independently in two other groups (Martin-Castellanos et al., 2005; Chikashige et al., 2006). Using multiple GFP- and mCherry-tagged markers for telomeres, the SPB, and the NE, we cytologically proved that Bqt2p specifically functions as a linkage component between telomeres and the SPB. It plays a key role in initiating telomere clustering by generating Sad1p foci proximate to the telomere foci upon pheromone sensing.

Correspondence to W. Zacheus Cande: zcande@uclink4.berkeley.edu

Abbreviations used in this paper: NE, nuclear envelope; SPB, spindle pole body.

The Journal of Cell Biology, Vol. 173, No. 6, June 19, 2006 845–851
http://www.jcb.org/cgi/doi/10.1083/jcb.200602152

Results and discussion

Identification of *bqt2/im295*, a mutant defective in heterochromatin reorganization during meiotic prophase by a visual screen

The dynamic reorganization of heterochromatin during sexual development in the fission yeast can be monitored using GFP-tagged Swi6p, a homologue of heterochromatin protein 1, which binds to all telomeres and centromeres as well as the silent mating type locus (which cannot be detected as a separate identity by light microscopy). During the horsetail stage, telomeres cluster at the leading edge of the nucleus adjacent to the SPB (Fig. 1 A, arrows), whereas centromeres are released into the interior of the nucleus. The attachment of telomeres to the SPB transmits mechanical forces from microtubule arrays to chromosomes, causing stretching and alignment of the homologues (Yamamoto and Hiraoka, 2001). Both telomere clustering and horsetail movement are important for homologous pairing (Ding et al., 2004).

To identify genes involved in telomere clustering, we developed a visual screen to search for mutants with aberrant GFP-Swi6p pattern during the horsetail stage. A strain expressing GFP-Swi6 (Pidoux et al., 2000) was mutagenized by random insertion of *ura4*$^+$ fragments (see Materials and methods). Because haploid cells have three chromosomes, 4–7 GFP-Swi6p foci are expected during the horsetail stage, depending on the extent of centromere pairing. From 18,000 *ura4*$^+$ insertional mutants (i.e., *im* mutants), we found several with defective telomere clustering, including *dos1*, *dos2*, *tel2*, *dhc1*, *taz1*, *trt1*, *eta2*, *matMi*, and *im295*. Among these, *im295* showed the most severe phenotype, as more than seven GFP-Swi6p dots were observed in >60% of the cells during meiotic prophase and stayed in the middle of the cells with little movement (Fig. 1, B and C). Furthermore, in >90% of the *im295* cells, the chromosome mass was not distended (Fig. 1, B and D). Therefore, both the telomere bouquet and the microtubule-driven chromosome stretching were severely disrupted in *im295* cells.

The *ura4*$^+$ insertion in *im295* was mapped to *spac1002.06c* (Fig. 1 E). This is an allele to *bqt2* (hereafter *bqt2*; Martin-Castellanos et al., 2005; Chikashige et al., 2006). The insertion replaced the 11th to 14th nucleotides of exon 2. The same meiotic defects in *bqt2-null* were observed in *im295*, and plasmids carrying this gene rescued the phenotype (unpublished data). Therefore, the *ura4*$^+$ insertion in *im295* caused the observed defects.

Bqt2p is required for linking telomeres to the meiotic SPB

We wanted to determine how lack of Bqt2p leads to defective telomere organization. The phenotype is not due to defects in sister chromatid cohesion or DNA replication because mutants found in our screen defective in these functions (*rec8* and *pop1*, respectively) have stretched chromosomes and moving leading edge. To determine whether the link between telomeres and the SPB was disrupted in *bqt2-null*, we labeled the SPB with Sad1p tagged with mCherry (Shaner et al., 2004) and telomeres with Taz1p tagged with GFP (Cooper et al., 1997). In wild type,

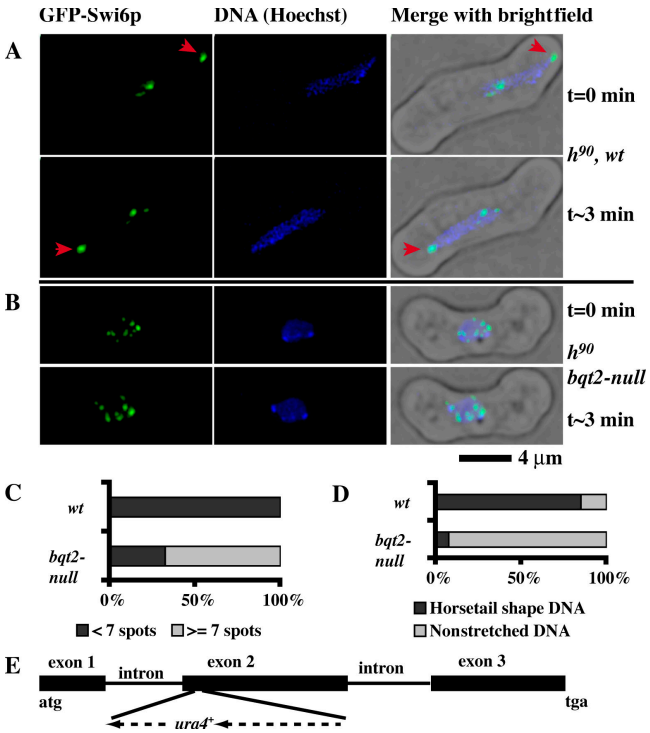

Figure 1. **Identification of *bqt2/im295* from a visual screen.** (A and B) Heterochromatin organization during the horsetail stage in wild type (wt; A) and in *bqt2/im295* (B). Live images were taken 20–24 h after inducing meiosis. The same cells were imaged after ~3 min to detect the movement of the nuclei. GFP-Swi6p is in green, and DNA stained with Hoechst is in blue. The red arrows indicate telomere foci at the leading edge of the moving nuclei. Bar, 4 μm. (C) Live cells were categorized with the number of GFP-Swi6p foci during meiotic prophase. 40 cells were checked totally. (D) Live cells were classified by the shape of their chromosome mass during meiotic prophase. 40 cells were checked totally. (E) The *ura4*$^+$ insertion in *im295* was mapped in the exon 2 of *bqt2*. The unspliced length of *bqt2*$^+$ is 512 bp. Exons and introns were drawn proportionally, but the ~1.8-kg bp *ura4*$^+$ insertion was not.

Sad1p and Taz1p colocalized as a single spot at the leading edge of the elongated nuclei (Fig. 2 A). In *bqt2-null*, however, multiple Taz1p foci were scattered in the middle of the cell, whereas a single Sad1p-mCherry spot moved to the cell tip (Fig. 2 B). Unlike in wild type (Fig. 2 H), the chromosome mass in *bqt2-null* is no longer stretched along with the single Sad1p foci driven by the microtubule arrays (Fig. 2, I and J), which was labeled with the GFP-tagged α-tubulin subunit Tub1p (Ding et al., 1998). Therefore, the meiotic SPB and telomeres were no longer connected in *bqt2-null* and, thus, the force generated by the microtubules failed to stretch chromosomes. To see if the disassociation of telomeres to the SPB in *bqt2-null* cells depends on the vigorous movement of the SPB, *dhc1-null* was used because there is only subtle movement in this mutant (Yamamoto et al., 1999). The *bqt2-null, dhc1-null* double mutants (Fig. 2 G) showed a similar Taz1p-GFP pattern to that observed in *bqt2-null* (Fig. 2 B) but not in *dhc1-null* (Fig. 2 F). Therefore, even without vigorous movement of the SPB, the connection between telomeres and the SPB is disrupted in Bqt2p-depleted cells.

After meiotic prophase, telomeres were detached from the SPB, and the telomere foci and DNA segregates equally in wild

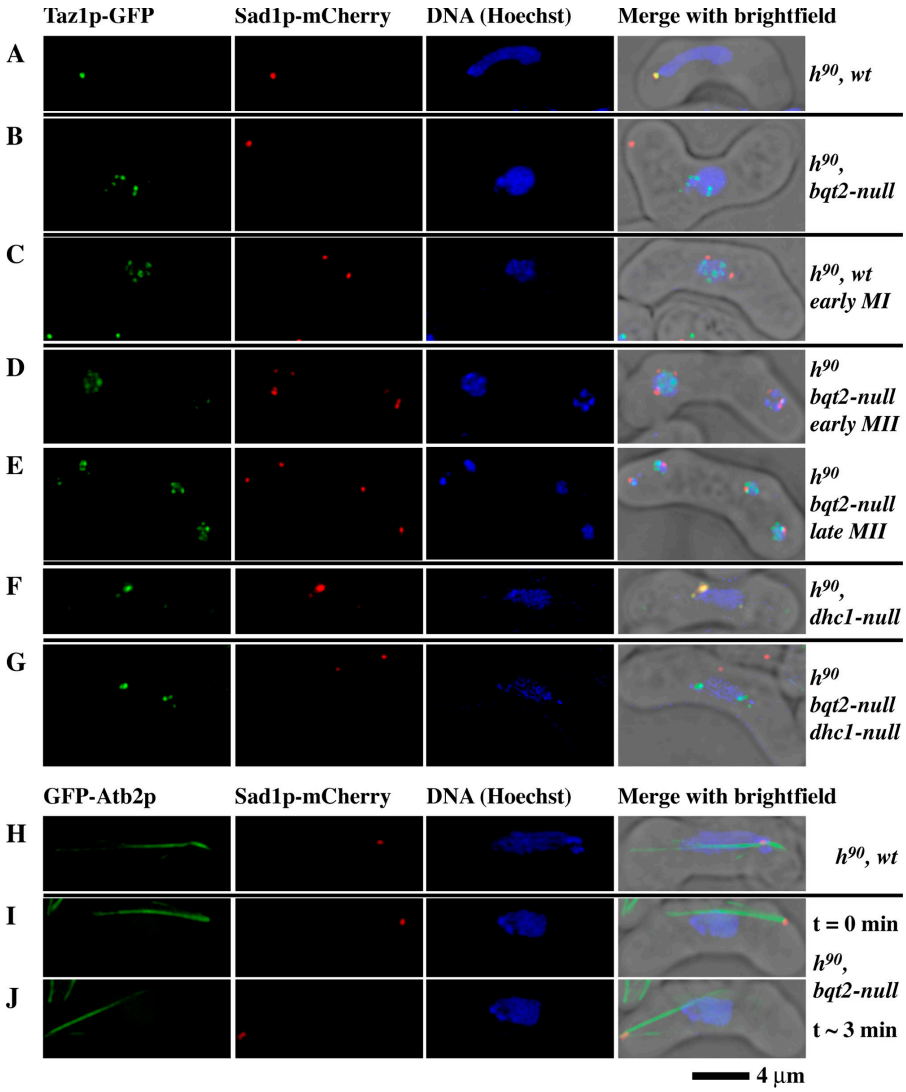

Figure 2. **Defective telomere clustering and chromosome segregation but normal SPB movement in *bqt2-null* cells.** Meiosis was induced, and cells were imaged after 20–26 h. (A–G) Normal telomere clustering in wild type (wt; A), abnormal telomere clustering in *bqt2-null* (B), wild type in early meiosis I (C), *bqt2-null* in early meiosis II (D) and in late meiosis II (E), abnormal telomere clustering in *dhc1-null* (F) and in *bqt2-null, dhc1-null* double mutant (G). Taz1-GFP is in green, Sad1-mCherry is in red, and DNA is in blue. (H–J) Normal microtubule behavior and DNA stretching was shown in wild type (H), and normal microtubule and SPB behavior but defective stretching of chromosome mass was shown in *bqt2-null* (I and J). GFP-Atb2p is in green, Sad1p-mCherry is in red, and DNA is in blue. Bar, 4 μm.

type (Fig. 2 C). However, nearly 40% of the *bqt2-null* showed abnormal distribution of chromosomes and Taz1p foci (Fig. 2, D and E). This phenotype is typical of mutants deficient in telomere clustering.

Bqt2p is required for generating Sad1p foci next to telomeres upon pheromone sensing but not for attachment of telomeres or the SPB to the NE

Telomeres start to cluster upon pheromone sensing before conjugation (Davey, 1998). Therefore, we analyzed telomere clustering upon pheromone response in *bqt2-null* cells using *mam2* deletion, which does not affect the response of h^+ to the pheromone release by h^- cells but blocks pheromone response of h^- cells and, consequently, the conjugation between h^+ and h^- cells. When homothallic h^{90}, *mam2-null* cells are starved, the cells switched to h^+ cells can sense the pheromone released by h^- cells, but not vice versa. Pheromone sensing induces a tip projection, called schmoo, necessary for cells to approach each other and conjugate. Schmoo and telomere clustering were blocked in starved heterothallic h^- cells because of the lack of pheromone (Fig. 3 A). In nearly 30% of the starved homothallic h^{90}, *mam2-null* population, cells showed either a single fully colocalized Sad1p and Taz1p foci (Fig. 3 B; 50 out of 193 cells) or more than one Sad1p spot that fully (Fig. 3 C; 6 out of 193 cells) or partially colocalized with Taz1p foci (Fig. 3 D; 26 out of 193 cells). This suggests that pheromone sensing generated Sad1p foci next to telomeres, which were pooled together by the microtubule arrays (Goto et al., 2001). The incomplete association of telomere foci and Sad1p foci suggests that the link between them is dynamic or not stable. In contrast, without Bqt2p, no telomere spots colocalized with the Sad1p foci, even in schmooing cells (Fig. 3 E; 137 cells checked). These results demonstrate that Bqt2p is essential for generating Sad1p foci next to the telomeres to initiate telomere clustering.

Although Bqt2p is essential for the association of telomeres and the SPB, it could function in one of two ways, either serving as a component of the linkage or coupling either telomeres or the SPB to the NE. In fission yeast, the SPB were observed to be free floating in some *cut11* mutant cells (West et al., 1998). In budding yeast, telomeres are detached from the

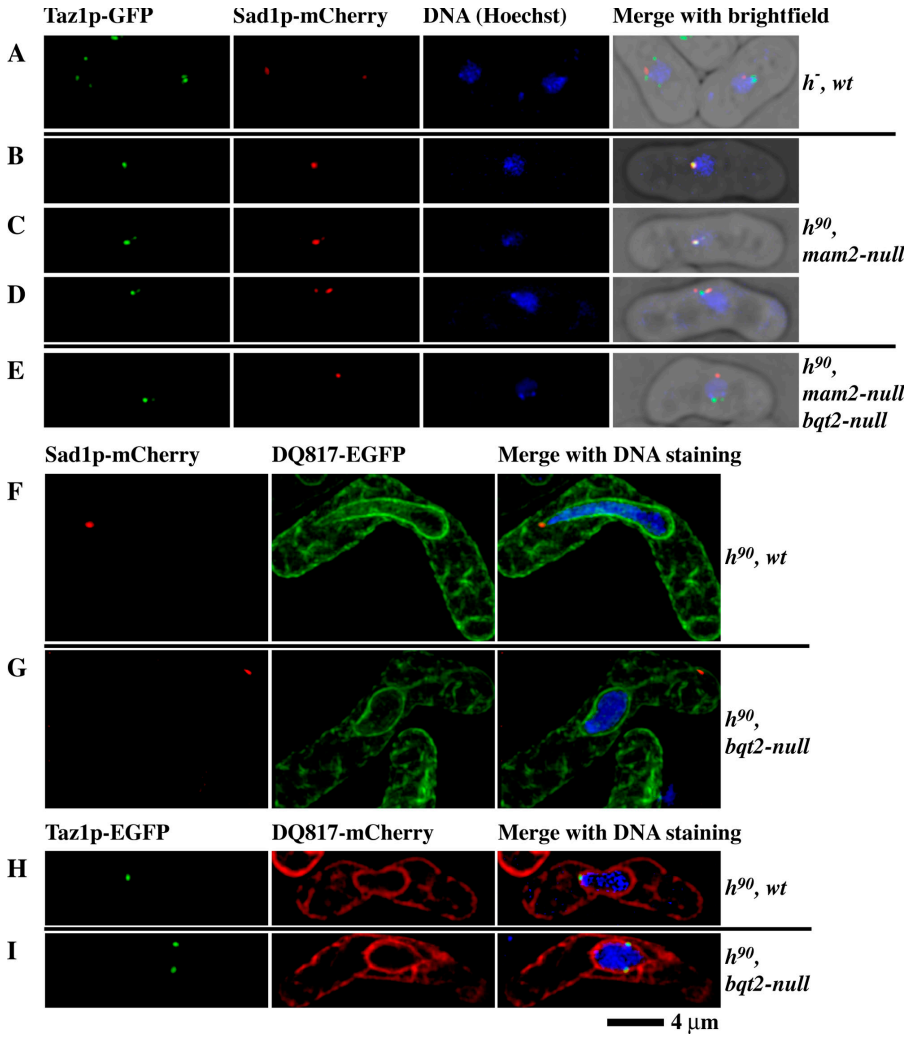

Figure 3. **Bqt2p is required for generating multiple Sad1p foci upon pheromone response but not for the attachment of telomeres and meiotic SPB to the NE.** (A) Heterothallic h^- cells upon starvation. 30 cells were checked. (B–D) Homothallic h^{90}, *mam2-null* cells upon starvation. 193 cells were checked. 50 cells had a similar pattern in B, 6 in C, and 26 in D. (E) Homothallic h^{90}, *mam2-null, bqt2-null* cells upon starvation. 137 cells were checked. (F and G) Wild-type (wt; F) and *bqt2-null* cells (G) with plasmid expressing D817-EGFP. Sad1p-mCherry is in red, D817-EGFP is in green, and DNA is in blue. (H and I) Wild-type (H) and *bqt2-null* cells (I) with plasmid expressing D817-mCherry. Single sections from the middle plane of the nucleus were analyzed. Taz1p-GFP is in green, D817-mCherry is in red, and DNA is in blue. Bar, 4 μm.

NE specifically upon meiosis entry in the *ndj1* mutant, which results in defective telomere clustering (Trelles-Sticken et al., 2000). To determine whether there was similar defect in *bqt2-null* during meiotic prophase, we used a membrane marker, D817, which is the NH_2-terminal 275 amino acid peptide of NADPH-cytochrome P450 reductase (Ding et al., 2000). In both wild type and *bqt2-null*, a single Sad1p spot remained at the tip of the NE (Fig. 3, F and G), but the NE adjacent to the tip in *bqt2-null* was stretched to form a thin line. From images of single middle z axis slices, all telomere foci were observed to attach to the inner NE in both wild type (Fig. 3 H) and *bqt2-null* (Fig. 3 I). Therefore, telomeres and the SPB were attached to NE membrane independent of Bqt2p during meiotic prophase. The disconnection of telomeres to the SPB must be due to a failure to establish a mechanical linkage between them.

Bqt2p localizes to the meiotic SPB, but depletion of Bqt2p is not required for dissolving telomere clustering

The endogenous Bqt2p was COOH-terminally tagged with GFP to check its expression and localization. Its expression was not observed in starved heterothallic h^- cells (Fig. 4 A). But upon sensing pheromone, when Bqt2p foci fully colocalized with Sad1p-mCherry in ~40% of the h^{90}, *mam2-null* population (Fig. 4, B and C), most of them were not schmooing yet. Therefore, pheromone induced Bqt2p expression. These results were consistent with the finding that Bqt2p was required to initiate telomere clustering. Compared with data showing partial colocalization of Taz1p and Sad1p in Fig. 3 D, these results also suggest that the colocalization of Bqt2p to Sad1p does not guarantee stable connection of all telomeres to the Sad1p foci.

As expected, Bqt2p-EGFP colocalized with the meiotic SPB during the horsetail stage. However, Bqt2p remained at the meiotic SPB at early meiosis I (8 out of 9 cells with same level of signal as that during meiotic prophase, and 1 with less intense signal) and until the end of meiosis II (23 out of 30 cells; few with same level of intense signal, and most with less intense signal; Fig. 4 D). Therefore, the disassociation of Bqt2p from the meiotic SPB is not required for dissolving telomere clustering at the end of meiotic prophase.

Ectopic expression of meiosis-specific proteins sometimes mimics meiotic cellular activity in vegetative cells. This is not the case for Bqt2p, as it was preferentially located in the nucleus but did not concentrate at the SPB when expressed in vegetative cells (Fig. 4 E). Therefore, other meiosis-specific factors may be required for docking Bqt2p to the SPB.

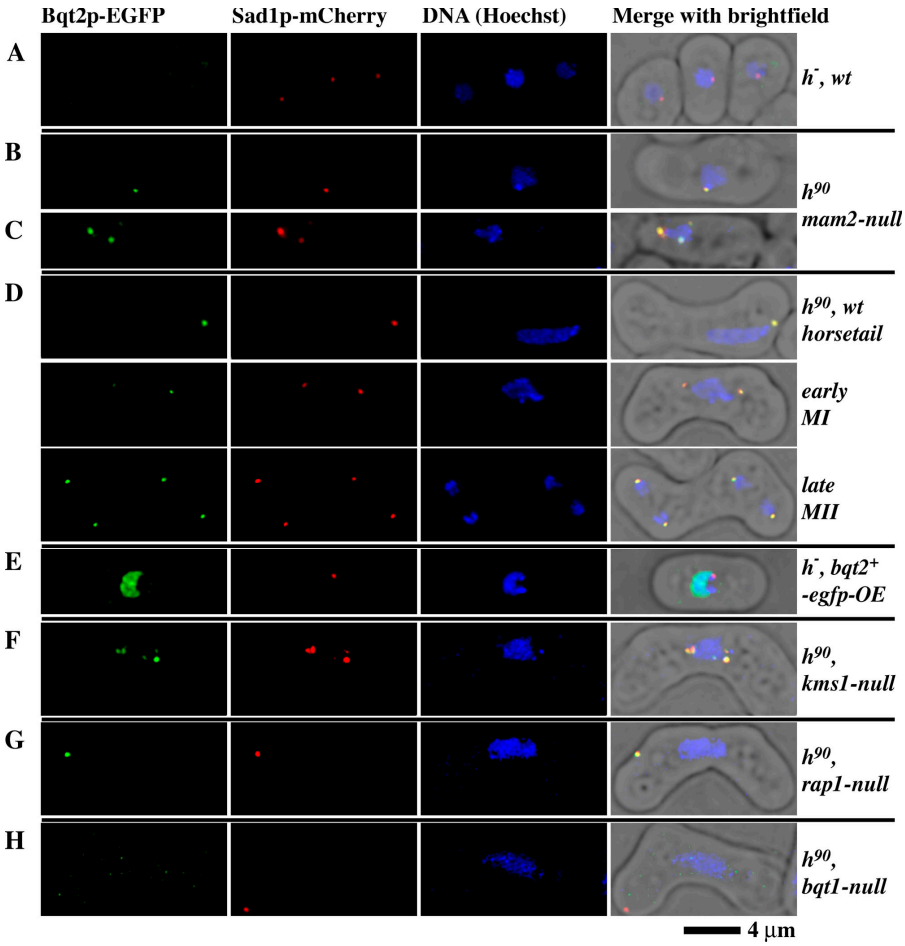

Figure 4. **Expression and localization of Bqt2p.** Fresh cells were either induced to undergo meiosis or starved in A–D and F–H, and fresh cells with plasmid *p157b2egfpOE* were streaked from minimal medium with thiamine to the one without thiamine to induce ectopic expression of Bqt2-EGFP in E. Bqt2p-EGFP is in green, Sad1p-mCherry is in red, and DNA is in blue. Bqt2p expression and localization upon starvation in control h^- wild type (wt; A), in h^{90}, *mam2-null* (B and C), in h^{90} *wt* during meiotic prophase, meiosis I and II (D), in h^- *[p157b2egfpOE]* after ectopic expression of Bqt2p-EGFP induced on medium without thiamine (E), in h^{90}, *kms1-null* (F), in h^{90}, *rap1-null* (G), and in h^{90}, *bqt1-null* (H). Bar, 4 μm.

Localization of Bqt2p to the meiotic SPB depends on Bqt1p but not on Rap1p and Kms1p

We analyzed the localization of Bqt2-GFP in several different mutants, including *kms1* (Shimanuki et al., 1997), *rap1* (Chikashige and Hiraoka, 2001; Kanoh and Ishikawa, 2001), and *bqt1* (Martin-Castellanos et al., 2005; Chikashige et al., 2006), all of which are defective in telomere clustering. Without Kms1p, multiple Sad1p foci are present, and Bqt2p colocalized to all the Sad1p foci (Fig. 4 F). Also, Bqt2p localized to the single Sad1p foci in the *rap1-null* (Fig. 4 G). These data demonstrate that Bqt2p localization to the Sad1p foci is independent of Kms1p, Rap1p, or telomeres. However, Bqt2p was no longer localized to the single Sad1-mCherry spot in *bqt1-null* (Fig. 4 H). Therefore, colocalization of Bqt2p to the meiotic SPB requires Bqt1p, and Bqt1p may link and/or stabilize the Bqt2p association with the Sad1p foci.

We have shown that Bqt2p is specifically essential for linking telomeres to the SPB and for transmitting force from the microtubule arrays to the chromosomes. Bqt2p is essential to initiating telomere clustering upon pheromone sensing, and it remains so after telomeres leave the SPB. Our observations agreed with the model for telomere clustering recently proposed by Chikashige et al. (2006). First, upon pheromone sensing, Bqt1p-Bqt2p binds to Sad1p. Once telomere binding proteins, such as Rap1p, interact with Bqt1p-Bqt2p, more Bqt2p-Bqt1p-Sad1p and other factors aggregate and attract Kms1p as well as other components of the microtubule cytoskeleton. However, other factors may be required to stabilize the connection between telomeres and the Sad1p foci. Kms1p may also function as one of these stabilizers because, in *kms1* mutants, there are multiple Sad1p foci not localized with the telomere foci (Shimanuki et al., 1997), which is totally different from the pattern in *dhc1* mutants (Fig. 2 F). Finally, the telomere foci are pooled together. Other forces, together with the forces generated by the cytoplasmic microtubules, are required to cluster telomeres. If this were not the case, we would expect that the Sad1p spot at the mitotic SPB would not colocalize with any telomere spots in *dhc1-null*, but this colocalization was observed (Fig. 2 F). Our hypothesis is consistent with the telomere bouquet formation in other organisms, which can occur without nuclear movement in meiotic prophase. At the end of meiotic prophase, the telomere bouquet is dissolved possibly by regulating the stabilizers for the linkage between telomeres and the SPB.

Materials and methods

General techniques, plasmid, and yeast strain collection

Methods and media for fission yeast were as described previously (Moreno et al., 1991). Molecular cloning was done as described previously (Sambrook and Russell, 2001).

The following plasmids were used in this study: *pUC18*, *p3BV*, *p4BV*, *p5BV*, *pFA6a-kanMX6*, *p17kanMX6*, *p13his5+*, *pKS-ura4*, *p16ura4+*, *p18hph*, *p31Tadh*, *p32Pnmt1*, *pEGFP*, *p42egfp*, *pFa-kanMX6*, *p46mCherry*,

p83This5⁺, *p86Tura4⁺*, *p107RgMh*, *p113RchMu*, *p157RgMh*, *p163RchMu*, *p157D817-egfp*, *p163D817-mCherry*, *p32bqt2*, and *p157b2egfpOE*.

The following fission yeast strains were used in this study: *YS127 [h⁹⁰, nmt41::gfp-swi6⁺::LEU2 (at ars1 locus), leu1-32, ura4D18], IM295 [im295 (ura4⁺ insertion in bqt2 from the screen) in TY127], TY104 [h⁹⁰, sad1-mCherry::ura4⁺, taz1-gfp::his5⁺, his5, ura4D18], YS783C3 [h⁹⁰, taz1-gfp::kanMX6, ade6-M216]* (provided by J.P. Cooper, Cancer Research UK, London, UK), *TY105 [h⁹⁰, sad1-mcherry::ura4⁺, bqt2-egfp::his5⁺, his5, ura4D18], TY108 [bqt2Δ::kanMX6 in TY104], TY109 [bqt1Δ::kanMX6 in TY105], TY110 [kms1Δ::kanMX6 in TY105], TY111 [mam2Δ::kanMX6 in TY105], TY112 [rap1Δ::kanMX6 in TY105], TY126 [h- sad1-mCherry::ura4⁺, taz1-gfp::his5⁺, his5, ura4D18], TY127 [bqt2Δ::kanMX6, mam2Δ::kanMX6, in TY104], TY128 [h-, sad1-mcherry::ura4⁺, bqt2-egfp::his5⁺, his5, ura4D18], TY129 [h⁹⁰, taz1-egfp::his5⁺, his5, ura4D18, {p163D817-mCherry}], TY130 [bqt2Δ::kanMX6 in TY129], TY131 [h⁹⁰, sad1-mcherry::ura4⁺, his5, ura4D18 {p157D817-egfp}], TY132 [bqt2Δ::kanMX6 in TY131], TY133 [dhc1Δ::hph in TY104], TY134 [dhc1Δ::hph in TY108], YY105 [[h⁹⁰, ura4D18, leu1-32, lys1⁺::mt1-gfp-atb2]* (provided by T. Toda, Y. Hiraoka, and D.Q. Ding, Kansai Advanced Research Center, Kobe, Japan), *TY135 [h⁹⁰, sad1-mCherry::ura4⁺, lys1⁺::nmt1-gfp-atb2]*, and *TY136 [h⁹⁰, sad1-mCherry::ura4⁺ bqt2Δ::kanMX6 lys1⁺::nmt1-gfp-atb2]*.

Plasmid construction

Fragment was amplified by PCR using *pUC18* as the template and two primers (5′-gaaagatatcggatccagacaaatgttggactagtggtttcttagacgtcaggtg-3′ and 5′-gaaagatatccagctgaattccaccatggaaatggtagatctggtaccatgtgagcaaaaggccagca-3′), restricted with EcoRV, and self-ligated to generate *p3BV*. Fragment was amplified by PCR using *pUC18* as the template and two primers (5′-gaaaagatctccatggaattcagctggtttcttagacgtcaggtg-3′ and 5′-gaaaagatctactagtaaaaagatatctggtaccatgtgagcaaaaggccagca-3′), restricted with BglII, and self-ligated to generate *p4BV*. Plasmid *p3BV* had a polylinker site (SpeI–BamHI–EcoRV–PvuII–EcoRI–BglII–KpnI), and *p4BV* had another one (PvuII–EcoRI–BglII–SpeI–EcoRV–KpnI). The *ARS* fragment from *pNMT41-TOPO* (Invitrogen) was amplified and cloned into the KpnI site of *p4BV*, generating *p5BV*. PCR was used to amplify the following fragments: *kanMX6*, *his5⁺*, *ura4⁺*, *Tadh*, *Pnmt1*, *egfp* (CLONTECH Laboratories, Inc.), *mCherry* (provided by R.Y. Tsien, University of California, San Diego, La Jolla, CA), and *hph* (hygromycin B–resistant gene; provided by C. Rasmussen, University of California, Berkeley, Berkeley, CA). If the fragments had some restriction sites that were the same as in the polylinker of *p1BV*, the two-step PCR overlap extension method was used to change one nucleotide and disrupt those sites but without altering amino acids. These PCR fragments were cloning into *p1BV* using EcoRV and EcoRI, generating the following plasmids: *p17knMX6*, *p18hph*, *p13his5⁺*, *p16ura4⁺*, *p31Tadh*, *p32Pnmt1*, *p42egfp*, and *p46mCherry*. All these plasmids have common sequences and restriction sites at the two sides. The SpeI–PvuII fragments carrying *his5⁺* and *ura4⁺* from *p13his5⁺* and *p16ura4⁺* were inserted to the SpeI–EcoRV site of *p31Tadh*, generating *p83This5⁺* and *p86Tura4⁺*, respectively. The SpeI–PvuII fragments carrying *egfp* and *mCherry* from *p42egfp*, *p46mCherry* were inserted to the SpeI–EcoRV sites of *p83This5⁺* and *p86Tura4⁺*, respectively, generating *p107RgMh*, *p113RchMu*. The SpeI–PvuII fragments carrying *gfp-Tadh-his5⁺* and *mCherry-Tadh-ura4⁺* from *p107RgMh* and *p113RchMu* were inserted to the SpeI–EcoRV sites of *p5BV*, generating *p157RgMh* and *p163RchMu*, respectively. The *D817* fragment together with its 5′ upstream promoter (~1.5 kb) was amplified from genomic DNA, restricted with BglII, and cloned into the BamHI site of *p157RgMh* and *p163RchMu*, respectively, generating *p157D817-egfp* and *p163D817-mCherry*. The *bqt2⁺* gene fragment was amplified, restricted with EcoRV and BglII, and inserted into the PvuII–BglII sites in *p32Pnmt1*, with the stop codon deleted, generating *p32bqt2⁺*. The *nmt1::bqt2⁺* fragment in *p32bqt2⁺* was cut out with BamHI and BglII and inserted into the BamHI site in *p157RgMh* to make *p157b2egfpOE*, in which *bqt2⁺* was COOH-terminally tagged with *egfp* and under the control of the inducible *nmt1*.

Insertional mutagenesis

Two primers with 18 bp specific to the *ura4⁺* gene and 30-bp random nucleotides were used to amplify the *ura4⁺* fragment. The PCR fragment with 30 bp of random flanking sequences on each side was transformed into the strain *h⁹⁰, nmt41::gfp-swi6⁺::LEU2, leu1-32, ura4D18*. Transformants were selected on Edinburgh minimal media without uracil. Stable insertional mutants were selected by replicating them, back and forth for twice, onto yeast extract plus supplement and Edinburgh minimal media without uracil. The colonies were replicated onto synthetic sporulation agar media to induce meiosis. GFP-Swi6p pattern was checked one by one after 20–24 h. Genomic DNA was isolated from the mutants and ligation-mediated suppression PCR (Strauss et al., 2001) was used to map the insertions.

Gene tagging, disruption, and expression

DNA fragments, such as *egfp*, *kanMX6*, and *Tadh1*, constructed in the plasmids were all flanked with two common cassettes (upstream, 5′-tgtctggatccgatatcggga-3′, and downstream, 5′-tcgcagctgaattccaccatg-3′; the three nucleotides underlined indicate the reading frame for reporter genes, in which the stop codons were deleted). The terminator had a stop codon next to the left cassette. Selection markers and combinations of reporter gene–*Tadh1*–selection marker between these two cassettes were used for gene disruption and COOH-terminal gene tagging, respectively. Two-step fusion PCR was used. One ~600-bp fragment upstream from the targeting site was amplified and was added with the 21 nucleotides of the upstream cassette at the 3′-end that was fused to the cassette. Another ~600-bp fragment downstream from the targeting site was amplified and was added with the 21 nucleotides of the upstream cassette at the 5′-end that was fused to the cassette. These two PCR products together with the corresponding modular vector for gene tagging and disruption were used as the templates to do fusion PCR. The fusion PCR products were transformed using the method described previously (Suga and Hatakeyama, 2001). The endogenous *his5⁺* was popped out using the method described previously (Iwaki and Takegawa, 2004). Strain *TY131* carrying the plasmid *p157b2egfpOE* was grown on appropriate minimal medium with 10 μM of thiamine and then streaked out to the same medium without thiamine to induce Bqt2p-GFP expression ectopically in mitotic cells (Forsburg, 1993).

Microscopy and live cell imaging

Live imaging was performed as described previously (Jin et al., 2002) with subtle modifications. Fresh cells grown on yeast extract plus supplement plates were induced into mating and meiosis by streaking cells onto synthetic sporulation agar plates. Cells were scraped off the plates 16–20 h later for checking pheromone response, 18–24 h later for checking cells during the horsetail stage, or 22–26 h later for checking cells during meiosis I and II. They were then suspended in 8 mg/ml Hoechst solution for at least 10 min and spotted onto a thin layer of 1% agarose (in 1/2 synthetic sporulation agar liquid medium) on slides. Then cells were covered and spread by an 18- × 18-mm coverslip. Images were collected using a wide-field inverted fluorescence microscope (IX70; Olympus) with a UPlanApo 100×, NA 1.35, oil-immersion objective (Olympus) using a charge-coupled device camera (CH350; Roper Scientific, Inc.) cooled to −35°C with DeltaVision image acquisition software (Applied Precision, Inc.). Serial sections in the z axis were acquired at 0.3-μm intervals, and data stacks were deconvolved using softWoRx deconvolution software (Applied Precision, Inc.). For presentation purposes, 2D projections were created from the 3D datasets using the DeltaVision image analysis software. To observe horsetail movement, images were taken at ~3-min intervals. Brightfield images were taken with six sections and 0.4-μm intervals. The images were processed and merged using Photoshop version 7.0 (Adobe).

We thank members of the Cande laboratory, especially Drs. M.S. Sagolla, L.C. Harper, and S.C. Dawson, for advice and comments on the manuscript; Drs. T. Toda, Y. Hiraoka, and D.Q. Ding for plasmids and strains; Dr. R.Y. Tsien for the *mCherry* gene; Dr. C. Rasmussen for the *hph* gene; Dr. J.P. Cooper for the *taz1-gfp* strains; and Y. Hiraoka for sharing data with us before publication.

The National Institutes of Health provided financial support for this research (grant R01-GM067992).

Submitted: 27 February 2006
Accepted: 16 May 2006

References

Chikashige, Y., and Y. Hiraoka. 2001. Telomere binding of the Rap1 protein is required for meiosis in fission yeast. *Curr. Biol.* 11:1618–1623.

Chikashige, Y., D.Q. Ding, Y. Imai, M. Yamamoto, T. Haraguchi, and Y. Hiraoka. 1997. Meiotic nuclear reorganization: switching the position of centromeres and telomeres in the fission yeast *Schizosaccharomyces pombe*. *EMBO J.* 16:193–202.

Chikashige, Y., C. Tsutsumi, M. Yamane, K. Okamasa, T. Haraguchi, and Y. Hiraoka. 2006. Meiotic proteins Bqt1 and Bqt2 tether telomeres to form the bouquet arrangement of chromosomes. *Cell.* 125:59–69.

Cooper, J.P., E.R. Nimmo, R.C. Allshire, and T.R. Cech. 1997. Regulation of telomere length and function by a Myb-domain protein in fission yeast. *Nature.* 385:744–747.

Davey, J. 1998. Fusion of a fission yeast. *Yeast.* 14:1529–1566.

Ding, D.Q., Y. Chikashige, T. Haraguchi, and Y. Hiraoka. 1998. Oscillatory nuclear movement in fission yeast meiotic prophase is driven by astral microtubules, as revealed by continuous observation of chromosomes and microtubules in living cells. *J. Cell Sci.* 111:701–712.

Ding, D.Q., Y. Tomita, A. Yamamoto, Y. Chikashige, T. Haraguchi, and Y. Hiraoka. 2000. Large-scale screening of intracellular protein localization in living fission yeast cells by the use of a GFP-fusion genomic DNA library. *Genes Cells.* 5:169–190.

Ding, D.Q., A. Yamamoto, T. Haraguchi, and Y. Hiraoka. 2004. Dynamics of homologous chromosome pairing during meiotic prophase in fission yeast. *Dev. Cell.* 6:329–341.

Forsburg, S.L. 1993. Comparison of *Schizosaccharomyces pombe* expression systems. *Nucleic Acids Res.* 21:2955–2956.

Goto, B., K. Okazaki, and O. Niwa. 2001. Cytoplasmic microtubular system implicated in de novo formation of a Rabl-like orientation of chromosomes in fission yeast. *J. Cell Sci.* 114:2427–2435.

Hagan, I., and M. Yanagida. 1995. The product of the spindle formation gene *sad1*$^+$ associates with the fission yeast spindle pole body and is essential for viability. *J. Cell Biol.* 129:1033–1047.

Harper, L., I. Golubovskaya, and W.Z. Cande. 2004. A bouquet of chromosomes. *J. Cell Sci.* 117:4025–4032.

Iwaki, T., and K. Takegawa. 2004. A set of loxP marker cassettes for Cre-mediated multiple gene disruption in *Schizosaccharomyces pombe*. *Biosci. Biotechnol. Biochem.* 68:545–550.

Jin, Y., S. Uzawa, and W.Z. Cande. 2002. Fission yeast mutants affecting telomere clustering and meiosis-specific spindle pole body integrity. *Genetics.* 160:861–876.

Kanoh, J., and F. Ishikawa. 2001. spRap1 and spRif1, recruited to telomeres by Taz1, are essential for telomere function in fission yeast. *Curr. Biol.* 11:1624–1630.

Lee, K.K., D. Starr, M. Cohen, J. Liu, M. Han, K.L. Wilson, and Y. Gruenbaum. 2002. Lamin-dependent localization of UNC-84, a protein required for nuclear migration in *Caenorhabditis elegans*. *Mol. Biol. Cell.* 13:892–901.

Martin-Castellanos, C., M. Blanco, A.E. Rozalen, L. Perez-Hidalgo, A.I. Garcia, F. Conde, J. Mata, C. Ellermeier, L. Davis, P. San-Segundo, et al. 2005. A large-scale screen in *S. pombe* identifies seven novel genes required for critical meiotic events. *Curr. Biol.* 15:2056–2062.

Miki, F., K. Okazaki, M. Shimanuki, A. Yamamoto, Y. Hiraoka, and O. Niwa. 2002. The 14-kDa dynein light chain-family protein Dlc1 is required for regular oscillatory nuclear movement and efficient recombination during meiotic prophase in fission yeast. *Mol. Biol. Cell.* 13:930–946.

Miki, F., A. Kurabayashi, Y. Tange, K. Okazaki, M. Shimanuki, and O. Niwa. 2004. Two-hybrid search for proteins that interact with Sad1 and Kms1, two membrane-bound components of the spindle pole body in fission yeast. *Mol. Genet. Genomics.* 270:449–461.

Moreno, S., A. Klar, and P. Nurse. 1991. Molecular genetic analysis of fission yeast *Schizosaccharomyces pombe*. *Methods Enzymol.* 194:795–823.

Nishikawa, S., Y. Terazawa, T. Nakayama, A. Hirata, T. Makio, and T. Endo. 2003. Nep98p is a component of the yeast spindle pole body and essential for nuclear division and fusion. *J. Biol. Chem.* 278:9938–9943.

Pidoux, A.L., S. Uzawa, P.E. Perry, W.Z. Cande, and R.C. Allshire. 2000. Live analysis of lagging chromosomes during anaphase and their effect on spindle elongation rate in fission yeast. *J. Cell Sci.* 113:4177–4191.

Sambrook, J., and D.W. Russell. 2001. Plasmids and their usefulness in molecular cloning. Molecular Cloning: A Laboratory Manual. Third Edition. Cold Spring Harbor Laboratory Press, NY. 1.32–1.162.

Scherthan, H. 2001. A bouquet makes ends meet. *Nat. Rev. Mol. Cell Biol.* 2:621–627.

Shaner, N.C., R.E. Campbell, P.A. Steinbach, B.N. Giepmans, A.E. Palmer, and R.Y. Tsien. 2004. Improved monomeric red, orange and yellow fluorescent proteins derived from *Discosoma* sp. red fluorescent protein. *Nat. Biotechnol.* 22:1567–1572.

Shimanuki, M., F. Miki, D.Q. Ding, Y. Chikashige, Y. Hiraoka, T. Horio, and O. Niwa. 1997. A novel fission yeast gene, *kms1*$^+$, is required for the formation of meiotic prophase-specific nuclear architecture. *Mol. Gen. Genet.* 254:238–249.

Strauss, C., J.H. Mussgnug, and O. Kruse. 2001. Ligation-mediated suppression-PCR as a powerful tool to analyse nuclear gene sequences in the green alga *Chlamydomonas reinhardtii*. *Photosynth. Res.* 70:311–320.

Suga, M., and T. Hatakeyama. 2001. High efficiency transformation of *Schizosaccharomyces pombe* pretreated with thiol compounds by electroporation. *Yeast.* 18:1015–1021.

Trelles-Sticken, E., M.E. Dresser, and H. Scherthan. 2000. Meiotic telomere protein Ndj1p is required for meiosis-specific telomere distribution, bouquet formation and efficient homologue pairing. *J. Cell Biol.* 151:95–106.

West, R.R., E.V. Vaisberg, R. Ding, P. Nurse, and J.R. McIntosh. 1998. *cut11*$^+$: a gene required for cell cycle-dependent spindle pole body anchoring in the nuclear envelope and bipolar spindle formation in *Schizosaccharomyces pombe*. *Mol. Biol. Cell.* 9:2839–2855.

Yamamoto, A., and Y. Hiraoka. 2001. How do meiotic chromosomes meet their homologous partners?: lessons from fission yeast. *Bioessays.* 23:526–533.

Yamamoto, A., R.R. West, J.R. McIntosh, and Y. Hiraoka. 1999. A cytoplasmic dynein heavy chain is required for oscillatory nuclear movement of meiotic prophase and efficient meiotic recombination in fission yeast. *J. Cell Biol.* 145:1233–1249.